Bisubstrate Inhibitor Approach for Targeting Mitotic Kinase Haspin

Katrin Kestav,[†] Darja Lavogina,[†] Gerda Raidaru,[†] Apirat Chaikuad,[‡] Alex N. Bullock,[‡] and Stefan Knapp*,[‡] Asko Uri,*,[†]

[†] University of Tartu, Institute of Chemistry, Ravila 14A, Tartu 50411, Estonia

[‡] University of Oxford, Nuffield Department of Clinical Medicine, Structural Genomics Consortium, Old Road Campus Research Building, Oxford OX3 7DQ, UK

*Corresponding authors.

Tel/fax: +372 737 5275, e-mail address: asko.uri@ut.ee (A. U.)

Tel/fax: ++44 1865 612933, e-mail address: stefan.knapp@sgc.ox.ac.uk (S. K.)

Keywords

Protein kinase, Haspin, Inhibitor, Histone H3, Conjugate of an Adenosine Analogue and a Peptide (ARC)

Abstract

In the recent decade, the basophilic atypical kinase Haspin has emerged as a key player in mitosis responsible for phosphorylation of Thr3 residue of Histone H3. Here, we report the construction of conjugates comprising an aromatic fragment targeted to the ATP-site of Haspin and a peptide mimicking the N-terminus of Histone H3 substrate of Haspin. The combination of effective solid phase synthesis procedures and a high throughput binding/displacement assay with affine fluorescent probes afforded the development of inhibitors with remarkable subnanomolar affinity towards Haspin. The selectivity profiles of novel conjugates were established by affinity studies with a model basophilic kinase (catalytic subunit of cAMP-dependent protein kinase) and by a commercial 1-point inhibition assay with 43 protein kinases.

Table of Contents Graphics

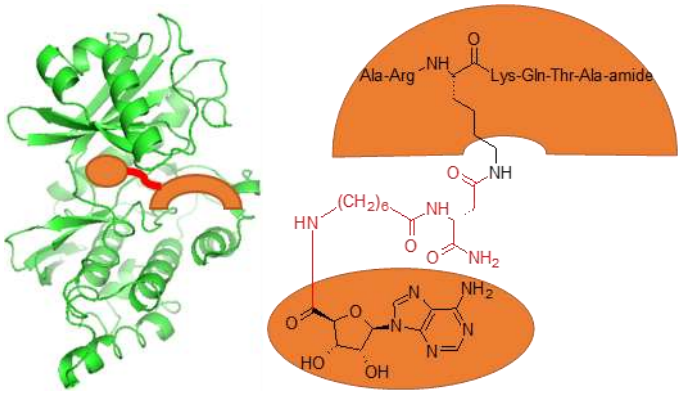

1. Introduction

Haspin kinase (GSG2) is a basophilic Ser/Thr protein kinase (PK[1]) that belongs to the group of atypical PKs.[1] Due to remarkable differences in its catalytic domain as compared to the 'canonical kinases' (*e.g.*, His651 is substituted in Haspin for the 'classical' catalytically important Lys responsible for chelation of ATP phosphate groups),[2,3] Haspin was initially considered to be an inactive pseudokinase. Recently, however, it has been demonstrated that Haspin is catalytically active and serves as an important player in mitosis.[4,5]

The only well-established physiological substrate of Haspin is Histone H3 which is phosphorylated by Haspin at Thr3 creating a docking site for Aurora B, which can then coordinate mitotic processes as a part of the chromosomal passenger complex.[6,7] The co-crystal structure of Haspin with Histone H3(1-7) peptide revealed a unique binding mode of the substrate peptide with U-shaped turn of the backbone and allowing the formation of interactions with both the N- and C-lobe of Haspin.[8] Such unusual conformation of the bound substrate peptide suggests that Haspin-selective compounds can be generated serving as probes and/or inhibitors of Haspin by targeting its substrate site.

So far, only two highly potent inhibitors of Haspin have been evolved, 5-iodotubercidin and LDN-192960 (Figure 1).[7,9] Both compounds target the ATP-site of Haspin, and do not utilize the unique structural and conformational features of the catalytic core of this PK. Also, the labelling of 5-iodotubercidin without loss of its affinity is synthetically challenging (our unpublished data), and no fluorescent probes for Haspin have so far been reported. The latter tools could potentially aid greatly both working out of quick biochemical assays as well as research of Haspin-related pathways in mitosis.

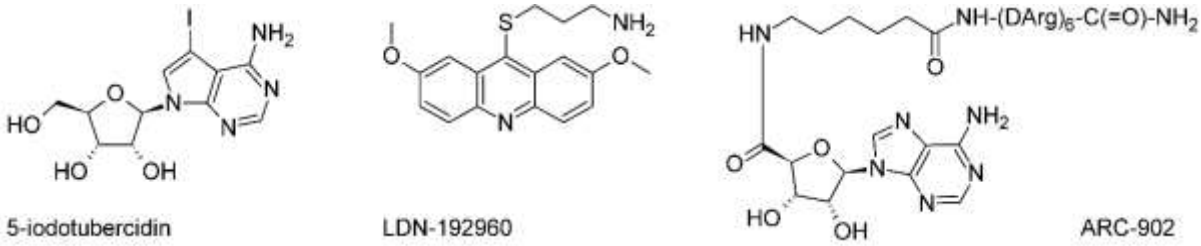

Figure 1. Structures of commercially available Haspin inhibitors (5-iodotubercidin, LDN-192960) and lead compound used in this study (ARC-902).

In this study, we set out to develop a novel class of Haspin-targeting scaffolds representing the bisubstrate-analogue inhibitors of PKs. Bisubstrate inhibitors comprise a fragment (nucleoside mimic) binding to the ATP-site of a PK and a fragment (peptide) binding to the protein substrate-site of a PK, fragments are joined by a linker chain (Figure 1).[10] The adenosine analogue-oligoarginine conjugates developed in our research group (generally termed ARCs) are 'assembled' using highly efficient and flexible solid phase synthesis procedures, enabling easy modification strategies and parallel syntheses of several compounds. The bisubstrate-analogue nature of such conjugates ideally translates into their increased affinity towards basophilic PKs (as compared to the affinities of individual fragments) as well as improved selectivity.[11-13]

In particular, we aimed at incorporation of Histone H3(1-7) peptide as the fragment targeting the protein substrate-site of Haspin. For that, we first established a quick and reliable binding/displacement assay with fluorescence polarization/anisotropy read-out, and used it for screening of a large set of previously reported ARCs that had been used for targeting basophilic PKs. Next, we established the possible ways

[1] Abbreviations: Abu, 4-aminobutanoic acid moiety; Adc, adenosine-4'-dehydroxymethyl-4'-carboxylic acid moiety; Ahx, 6-aminohexanoic acid moiety; AMSE, 5-(2-aminopyrimidin-4-yl)-selenophene-2-carboxylic acid moiety; AMTH, 5-(2-aminopyrimidin-4-yl)-thiophene-2-carboxylic acid moiety; ARC, adenosine analogue-oligoarginine conjugate; DAP, diaminopropionic acid moiety; H9, *N*-aminoethyl-5-isoquinolinesulfonamide moiety; Inp, isonipecotic acid (4-piperidinecarboxylic acid) moiety; Myr, myristoyl; PIPY, 4-(piperazin-1-yl)-7H-pyrrolo[2,3-d]pyrimidine moiety; PK, protein kinase; PKAc, catalytic subunit of cAMP-dependent protein kinase; PYB, 3-(pyridin-4-yl)benzoic acid moiety; TIBI, 4,5,6,7-tetraiodo-1H-benzimidazole moiety; Tnx, tranexamic acid (trans-4-(aminomethyl)cyclohexanecarboxylic acid) moiety.

for linking the nucleoside mimics to the Histone H3(1-7) peptide and performed the synthesis of several new ARCs. The affinity of the conjugates towards Haspin and a model basophilic kinase was established in the binding/displacement assay, and two novel compounds were profiled towards a panel of 43 PKs for wider selectivity studies.

2. Results and Discussion

2.1. Binding Assay with Fluorescent ARCs

We started the study by choosing a set of structurally diverse fluorescent ARC-based probes that had previously been used for targeting basophilic PKs to be screened towards Haspin in a biochemical binding assay[14] (detailed structures of the probes are given in Supplementary Table S1). The initially chosen ARCs had low nanomolar or subnanomolar dissociation constants (K_D values) towards their reported PK targets (cAMP- and cGMP-dependent PKs, Rho kinase, *etc*) and relatively broad selectivity profiles according to studies on commercial PK panels.[13-17] Hence, we expected that some of these probes would be applicable for establishment of quick biochemical binding/displacement assays for Haspin.

Titration of the probes with Haspin protein revealed the affinity of the probes towards the kinase; the calculated values of the dissociation constant K_D together with the factor Q (ratio of fluorescence intensities of Haspin-bound *and* free probe) are reported in Table 1. The highest affinity comprised inhibitors that harboured conjugates ARC-1042 and ARC-1081 incorporating adenosine-4'-dehydroxymethyl-4'-carboxylic acid moiety (Adc) as the PK ATP-site targeting fragment and (DArg)$_6$-DLys as the PK protein substrate-site targeting fragment linked by two flexible 6-aminohexanoic acid moieties (Ahx) and a chiral DArg spacer. Irrespective of the fluorescent dye (TAMRA or Cy3B) attached to the C-termini of conjugates *via* the side-chain of DLys, K_D values for Haspin of 1 nM were obtained for ARC-1042 and ARC-1081.

Table 1. Values of the dissociation constant K_D and the intensity ratio Q of fluorescent probes established in the binding assay by titration with Haspin

Nr	Schematic Structure	K_D, nM**	Q**
ARC-583	Adc-Ahx-DArg$_6$-DLys*(TAMRA)-NH_2	2.0 (0.8)	1.4 (0.1)
ARC-669	AMTH-Ahx-DArg-Ahx-DArg$_6$-DLys*(TAMRA)-NH_2	9.2 (2.5)	3.7 (0.5)
ARC-1042	Adc-Ahx-DArg-Ahx-DArg$_6$-DLys*(TAMRA)-NH_2	0.91 (0.28)	3.7 (0.9)
ARC-1059	H9-$(CH_2)_5$-C(=O)-DArg$_6$-DLys*(TAMRA)-NH_2	2.0 (0.3)	3.1 (0.1)
ARC-1081	Adc-Ahx-DArg-Ahx-DArg$_6$-DLys*(Cy3B)-NH_2	1.0 (0.2)	3.1 (0.8)
ARC-1144	AMSE-Ahx-DArg-Ahx-DArg$_6$-DLys*(TAMRA)-NH_2	23 (8)	4.5 (0.5)

Q was calculated as the ratio of fluorescence intensities of Haspin-bound *versus* free probe. * points to the DLys residue whose side-chain amino group was used for the attachment of the fluorescent dye; **standard error values are given in brackets (N = 2 or more).

2.2. Displacement Assay and Thermal Shift Assay with Non-Fluorescent ARCs

Next, displacement of the probe ARC-1081 from its complex with Haspin was performed by a larger set of non-fluorescent ARCs representing variable structural scaffolds to identify inhibitors that could serve as starting points (lead compounds) for the design of Haspin-selective compounds (detailed structures of compounds are given in Supplementary Table S1). The screening set consisted of previously reported ARCs or their analogues[15,16,18-20] comprising different ATP-site-targeting fragments; other structural variations included different chirality (D or L) and number of Arg residues (2, 4, 6 or 8) and linkers (1 or 2), incorporation of a chiral spacer between the two linker moieties, and attachment of a fatty acid moiety. The schematic structures of compounds and the assay results are given in The data revealed that the affinity of compounds towards Haspin strongly depends on the number of Arg residues; in general, the addition of two Arg residues approximately leads to the increase of affinity of up to two orders of magnitude (*e.g.*, series ARC-1034 → ARC-582 → ARC-902). Still, eight DArg residues in the peptidic part did not improve the affinity of the conjugate compared to the compound with six DArg residues (ARC-1090 *versus* ARC-902). In addition, DArg seemed to be preferred over the

L-isomer in the peptidic fragment of the compounds (ARC-902 *versus* ARC-341); however, the chirality of spacer between the linkers does not affect the affinity of conjugates towards Haspin (ARC-1012 *versus* ARC-1038).

Table 2.

The data revealed that the affinity of compounds towards Haspin strongly depends on the number of Arg residues; in general, the addition of two Arg residues approximately leads to the increase of affinity of up to two orders of magnitude (*e.g.*, series ARC-1034 → ARC-582 → ARC-902). Still, eight DArg residues in the peptidic part did not improve the affinity of the conjugate compared to the compound with six DArg residues (ARC-1090 *versus* ARC-902). In addition, DArg seemed to be preferred over the L-isomer in the peptidic fragment of the compounds (ARC-902 *versus* ARC-341); however, the chirality of spacer between the linkers does not affect the affinity of conjugates towards Haspin (ARC-1012 *versus* ARC-1038).

Table 2. Values of the dissociation constant K_d established in the displacement assay and values of the thermal shift ΔT_m of non-fluorescent compounds with Haspin

Nr	Schematic Structure	K_d, nM**	ΔT_m, °C**
ARC-1010	Adc-Ahx	over 15000	ND
ARC-1034	Adc-Ahx-DArg_2-NH_2	3400 (400)	4.5 (0.1)
ARC-582	Adc-Ahx-DArg_4-NH_2	110 (8)	ND
ARC-902	Adc-Ahx-DArg_6-NH_2	2.6 (0.3)	8.6 (0.2)
ARC-1090	Adc-Ahx-DArg_8-NH_2	9.0 (1.1)	ND
ARC-341	Adc-Ahx-LArg_6-NH_2	40 (4)	5.7 (0.1)
ARC-342	Adc-Ahx-LArg_6-LLys-NH_2	33 (2)	ND
ARC-1012	Adc-Ahx-DLys-Ahx-DArg_2-NH_2	2000 (200)	4.6 (0.1)
ARC-1038	Adc-Ahx-LLys-Ahx-DArg_2-NH_2	2000 (100)	4.2 (0.1)
ARC-1041	Adc-Ahx-DArg-Ahx-DArg_6-DLys-NH_2	0.24 (0.11)	ND
ARC-1176	AMTH-Ahx-DArg-NH_2	over 15000	ND
ARC-1102	AMTH-Ahx-DLys-Ahx-DArg_2-NH_2	over 15000	2.8 (0.0)
ARC-668	AMTH-Ahx-DArg-Ahx-DArg_6-dLys-NH_2	15 (3)	8.0 (0.1)
ARC-1141	AMTH-Ahx-DAla-DArg_6-DLys-Gly	16 (3)	6.0 (0.1)
ARC-1143	AMTH-Ahx-DAla-DArg_6-DLys*(Myr)-Gly	66 (5)	ND
ARC-1197	AMTH-Ahx-DArg-Ahx-DArg_6-DLys*(-C(=O)-$(CH_2)_7$-C(=O)-DArg_6-NH_2)-NH_2	4.7 (0.5)	ND
ARC-3009	H9-C(=O)-CH_2-NH-CH_2-C(=O)-DArg_2-NH_2	over 15000	1.1 (0.1)
ARC-3010	H9-C(=O)-CH_2-NH-CH_2-C(=O)-DArg_6-NH_2	800 (160)	2.0 (0.1)
ARC-903	H9-$(CH_2)_5$-C(=O)-DArg_6-NH_2	37 (3)	ND
ARC-1408	PIPY-C(=O)-$(CH_2)_7$-C(=O)-DArg-Ahx-DArg-NH_2	3700 (600)	3.9 (0.0)
ARC-1411	PIPY-C(=O)-$(CH_2)_7$-C(=O)-DArg_6-DLys-NH_2	11 (2)	7.8 (0.1)
ARC-684	PYB-Ahx-DArg-Ahx-DArg_6-DLys-NH_2	17 (3)	5.7 (0.1)
ARC-685	PYB-Ahx-DArg-Ahx-DArg_6-DLys*(Myr)-NH_2	390 (50)	2.8 (0.1)
ARC-3125	TIBI-CH_2-C(=O)-Ahx-DArg_6-DLys-NH_2	0.56 (0.09)	10.1 (0.1)
-	DArg_9-NH_2	over 15000	ND

The compounds are listed in alphabetical order according to their ATP-site binding fragments. * points to the DLys residue whose side-chain amino group was used for the attachment of the fragment in brackets; **standard error values are given in brackets (N = 2 or more).

In Adc-comprising compounds with two Arg residues, introduction of the second linker did not result in remarkable gain of affinity (ARC-1034 *versus* ARC-1012); for their counterparts with six Arg, however, introduction of the second linker increased the affinity of conjugates 10-fold (ARC-902 *versus* ARC-1041). In AMTH-containing compounds, no effect of the second linker on the affinity of conjugates

towards Haspin could be observed (ARC-668 *versus* ARC-1141). The effect of introduction of a myristoyl group (Myr) was also not uniform: no change of affinity was observed for compounds containing AMTH as the ATP-site targeting fragment (ARC-1141 *versus* ARC-1143), but the affinity decreased upon incorporation of Myr in compounds containing 3-(pyridin-4-yl)benzoic acid moiety (PYB; ARC-684 *versus* ARC-685).

Surprisingly, the ATP-site targeting fragment itself (AMTH, Adc, PYB, N-aminoethyl-5-isoquinolinesulfonamide moiety (H9), 4-(piperazin-1-yl)-7H-pyrrolo[2,3-d]pyrimidine moiety (PIPY) or 4,5,6,7-tetraiodo-1H-benzimidazole moiety (TIBI)) did not seem to have significant impact on affinity (the lower affinity of H9-containing compounds could rather be attributed to the different linker structure, as the H9-containing conjugate ARC-903 showed relatively high affinity to Haspin).

Additionally, Adc fragment with a linker (ARC-1010), and $_{D}Arg_9$ peptide were tested. Expectedly, these fragments separately at the highest tested concentration were unable to fully displace the probe from its complex with the kinase; therefore, it was demonstrated that in order to obtain the considerable affinity towards Haspin, the linking of these fragments was indeed required.

For characterization of most of the aforementioned inhibitors, the thermal shift assay which measures rge stabilization of Haspin upon binding to the compounds was also used (The data revealed that the affinity of compounds towards Haspin strongly depends on the number of Arg residues; in general, the addition of two Arg residues approximately leads to the increase of affinity of up to two orders of magnitude (*e.g.*, series ARC-1034 → ARC-582 → ARC-902). Still, eight $_{D}$Arg residues in the peptidic part did not improve the affinity of the conjugate compared to the compound with six $_{D}$Arg residues (ARC-1090 *versus* ARC-902). In addition, $_{D}$Arg seemed to be preferred over the $_{L}$-isomer in the peptidic fragment of the compounds (ARC-902 *versus* ARC-341); however, the chirality of spacer between the linkers does not affect the affinity of conjugates towards Haspin (ARC-1012 *versus* ARC-1038).

Table 2). In general, the results of displacement assay and thermal shift assay agreed well (*i.e.*, the larger temperature shift ΔT_m values corresponded to lower IC_{50} values reflecting higher affinity) with the exception of compounds ARC-685 and ARC-3010 whose ΔT_m values were smaller than expected for potent inhibitors.

2.3. Design of Novel Compounds

Next, we proceeded to design of novel conjugates targeting Haspin and comprising a Histone H3(1-7) peptide. Based on the established structure-affinity relationship, we chose Adc and AMTH as the ATP-site targeting fragments. In addition, from the available Haspin:Histone H3(1-7) co-crystal, we predicted two positions in the structure of Histone H3(1-7) where nucleoside mimics of ARCs could be linked to: the proximity of the N-terminus of peptide, and the proximity of the phosphorylatable residue Thr3 (Figure 2). Overall, this approach resulted in generation of two sets of novel compounds (detailed structures of compounds are given in Supplementary Table S1).

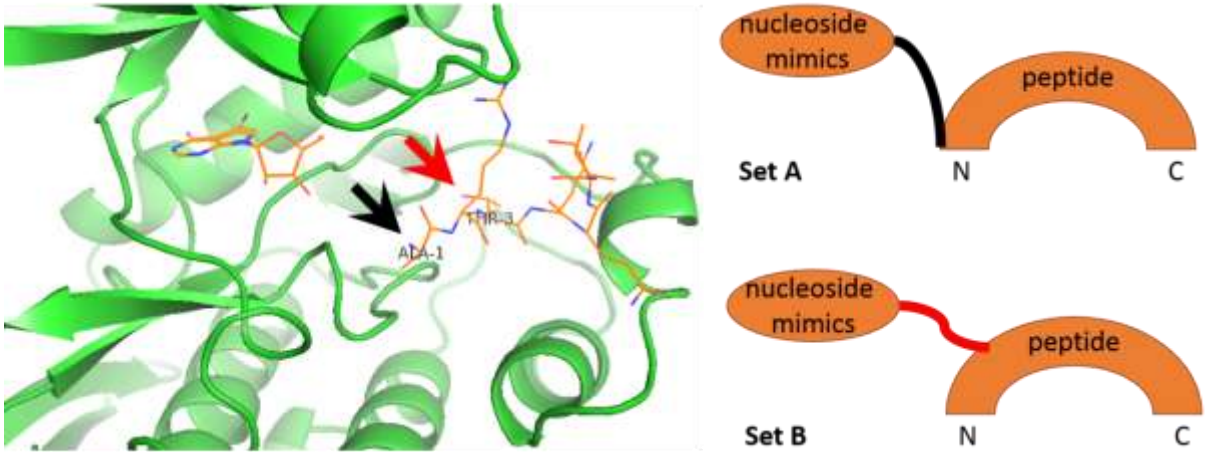

Figure 2. Principles of linkage of nucleoside mimics and Histone H3(1-7) peptide within the structure of novel conjugates. Left, co-crystal of Haspin with Histone H3(1-7) and 5-iodotubercidin (PDB 4OUC). PK is indicated as green cartoon, Histone H3(1-7) and 5-iodotubercidin as orange lines. The arrows show two possible positions in the structure of Histone H3(1-7) where the nucleoside mimics of ARCs could be linked to. Right, simplified scheme of linkage in compounds belonging to Set A or Set B.

2.3.1. Set A: Linkage *via* N-Terminal Region of Histone H3(1-7) (Compounds 1-13)

Two strategies were chosen for linkage of nucleosidic moiety to the N-terminal region of Histone H3(1-7) or slightly modified sequence (Table 3). In the first case, Ala1 was replaced with DLys, and AMTH moiety was connected *via* a linker to the side-chain of DLys (as the side-chain of Ala1 in the Histone H3(1-7) co-crystal was pointing away from the ATP-site, the change of chirality L → D was expected to 'flip' the position of this side-chain). In the second case, Ala1 was replaced with D-diaminopropionic acid moiety (DDap), and nucleosidic moiety was connected *via* a linker directly to the N-terminus of the peptide.

The compounds of Set A contained AMTH as the ATP-site targeting fragment and had an amidated C-termini. Amidation was necessary for both the synthetic rationale and improvement of affinity of the conjugates as it masked the negative charge of the C-terminal carboxylate. The structural variations in the compound set included acylation of N-terminus of Histone H3(1-7)-like peptide, and incorporation of different linkers between the nucleosidic moiety and Histone H3(1-7)-like peptide. Additionally, Arg_6 motif (L or D) was added in some cases to the N- or C-terminus of Histone H3(1-7)-like peptide; the rationale behind such structural variation was incorporation of the positive charges to the inhibitor, which were expected to increase the affinity of novel compounds to basophilic Haspin. It was also presumed that oligoarginine as the cell plasma membrane-penetrative peptide sequence[21] could facilitate internalization of developed compounds into live cells in future studies.

2.3.2. Set B: Linkage *via* Phosphorylatable Region of Histone H3(1-7) (Compounds 14-21)

Again, two strategies were used for linkage of nucleosidic moiety to the phosphorylatable region of Histone H3(1-7) or slightly modified sequence of the peptide (Table 3). In the first case, Thr3 was replaced with LAsp, and nucleosidic moiety was connected *via* linker and side-chain of chiral spacer (DLys) to the side-chain of LAsp. On synthetic rationale, the N-terminus of Histone H3(1-7)-like peptide was acylated, and Thr6 of Histone H3(1-7) was replaced with LAla. In the second case, Thr3 was replaced with LLys, and nucleosidic moiety was connected *via* linker(s) and/or side-chain of chiral spacer (DAsp) to the side-chain of LLys.

Most of the novel compounds of Set B contained Adc as the ATP-site targeting fragment; in one case, AMTH was substituted for Adc. The structural variations in the compound set included incorporation of different linkers between Adc moiety and Histone H3(1-7)-like peptide. Again, Arg_6 motif (L or D) was added in some cases to the N- or C-terminus of Histone H3(1-7)-like peptide. All of the novel compounds of the Set B also had amidated C-termini.

2.4. Biochemical Characterization of Novel Compounds

2.4.1. Affinity Studies

The affinities of both sets of novel compounds were characterized in displacement assay with Haspin and the fluorescent probe ARC-1081. As reference compounds, the previously described conjugates ARC-1141 (contains AMTH moiety) and ARC-902 (contains Adc moiety) and a well-known inhibitor of Haspin 5-iodotubercidin were used. In order to establish whether the novel compounds were potentially selective towards Haspin, the displacement assay was also performed with a reference PK, catalytic subunit of cAMP-dependent protein kinase (PKAc). The latter PK is also basophilic, and several of the starting compounds (The data revealed that the affinity of compounds towards Haspin strongly depends on the number of Arg residues; in general, the addition of two Arg residues approximately leads to the increase of affinity of up to two orders of magnitude (*e.g.*, series ARC-1034 → ARC-582 → ARC-902). Still, eight DArg residues in the peptidic part did not improve the affinity of the conjugate compared to the compound with six DArg residues (ARC-1090 *versus* ARC-902). In addition, DArg seemed to be preferred over the L-isomer in the peptidic fragment of the compounds (ARC-902 *versus* ARC-341);

however, the chirality of spacer between the linkers does not affect the affinity of conjugates towards Haspin (ARC-1012 *versus* ARC-1038).

Table 2) had initially been developed as inhibitors of PKAc. The determined affinities of the new compounds are presented in Table 3 and some representative displacement curves are shown in Supplementary Figure S1.

Importantly, the dissociation constant K_d value calculated from the displacement IC_{50} value for reference compound 5-iodotubercidin in assay with Haspin was very well comparable to the inhibitory potency of the compound (IC_{50} value of 3-9 nM reported for inhibition assay performed at ATP concentration close to K_M).[6,7] The K_d value for starting compound ARC-902 in assay with PKAc was also in a very good agreement with the previously published data (inhibition constant K_i value of 3.2 nM).[18]

All of the compounds in set A possessed lower affinity towards Haspin than the reference compound ARC-1141. Notably, the incorporation of Arg_6 motif resulted in dramatic increase of affinity of conjugates (*e.g.*, K_d value of 120 nM for Compound 6 *versus* K_d value of 13000 nM for Compound 5). The acylation of the N-terminus of Histone H3(1-7)-like peptide, on the other hand, caused 2-fold drop of affinity of conjugates towards Haspin (K_d value of over 15000 for Compound 1 *versus* K_d value of 8800 nM for Compound 4). Out of compounds without Arg_6 motif, the best affinity towards Haspin was revealed by Compound 8 (K_d value of 5200 nM). Still, variation of the linker structure of Compound 8 (as in Compounds 9-13) demonstrated that the length and flexibility strongly affected binding of conjugates to Haspin.

Remarkably, for all conjugates of set A except Compound 9 the selectivity towards Haspin *versus* PKAc was improved one to three orders of magnitude as compared to the reference compound ARC-1141. The increase of selectivity was also not pronounced in case of Compound 8, which pointed to fact that conjugation of AMTH moiety *via* a linker directly to the N-terminal part of Histone H3(1-7)-like peptide was not profitable from the point of gaining selectivity. Notably, from the comparison of selectivity indices of compounds 6 and 7 *versus* Compound 2 and 3, it was evident that the positioning of Arg_6 motif relative to the N- *versus* C-terminus of Histone H3(1-7)-like peptide served as selectivity determinant: N-terminal Arg_6 was preferred by PKAc, whereas C-terminal Arg_6 was preferred by Haspin.

Table 3. Values of the dissociation constant K_d and selectivity index of novel conjugates established in the displacement assays with Haspin and PKAc

Nr	Schematic Structure	K_d, nM** Haspin	K_d, nM** PKAc	Selectivity Index***
ARC-1141	AMTH-Ahx-DAla-DArg_6-DLys-Gly	16 (3)	0.06 (0.02)	0.004
ARC-902	Adc-Ahx-DArg_6-NH_2	2.6 (0.3)	2.7 (0.4)	1
-	5-iodotubercidin	3.9 (0.4)	over 15000	over 4000
Set A				
1	AMTH-Gly-[Ac-DLys*-LArg-LThr-LLys-LGln-LThr-LAla-NH_2]	over 15000	over 15000	ND
2	AMTH-Gly-[Ac-DArg_6-DLys*-LArg-LThr-LLys-LGln-LThr-LAla-NH_2]	130 (20)	89 (6)	0.7
3	AMTH-Gly-[Ac-LArg_6-DLys*-LArg-LThr-LLys-LGln-LThr-LAla-NH_2]	82 (10)	39 (3)	0.5
4	AMTH-Gly-[DLys*-LArg-LThr-LLys-LGln-LThr-LAla-NH_2]	8800 (1000)	5800 (600)	0.7
5	AMTH-Abu-[DLys*-LArg-LThr-LLys-LGln-LThr-LAla-NH_2]	13000 (2000)	5000 (500)	0.4
6	AMTH-Abu-[DLys*-LArg-LThr-LLys-LGln-LThr-LAla-DArg_6-NH_2]	120 (10)	570 (40)	5
7	AMTH-Abu-[DLys*-LArg-LThr-lLys-LGln-LThr-LAla-LArg_6-NH_2]	150 (10)	550 (40)	4
8	AMTH-Ahx-[DDAP-LArg-LThr-LLys-LGln-LThr-LAla-NH_2]	5200 (700)	330 (20)	0.06
9	AMTH-Aoc-[DDAP-LArg-LThr-LLys-LGln-LThr-LAla-NH_2]	over 15000	51 (3)	below 0.004
10	AMTH-DPro-Gly-[DDAP-LArg-LThr-LLys-LGln-LThr-LAla-NH_2]	over 15000	over 15000	ND
11	AMTH-LPro-Gly-[DDAP-LArg-LThr-LLys-LGln-LThr-LAla-NH_2]	over 15000	over 15000	ND
12	AMTH-Inp-Gly-[DDAP-LArg-LThr-LLys-LGln-LThr-LAla-NH_2]	9500 (1300)	3800 (200)	0.4

13	AMTH-Tnx-Gly-[DDAP-LArg-LThr-LLys-LGln-LThr-LAla-NH_2]	over 15000	over 15000	ND
Set B				
14	Adc-Ahx-DLys*[Ac-LAla-LArg-LAsp*-LLys-LGln-LAla-LAla-NH_2]-NH_2	5200 (700)	1700 (100)	0.3
15	Adc-Ahx-DAsp*[LAla-LArg-LLys*-LLys-LGln-LThr-LAla-NH_2]-NH_2	170 (40)	1600 (300)	9
16	Adc-Ahx-DAsp*[LAla-LArg-LLys*-LLys-LGln-LThr-LAla-LArg_6-NH_2]-NH_2	0.42 (0.14)	38 (4)	90
17	Adc-Ahx-DAsp*[LAla-LArg-LLys*-LLys-LGln-LThr-LAla-DArg_6-NH_2]-NH_2	0.88 (0.15)	27 (3)	30
18	Adc-Ahx-Abu-[LAla-LArg-LLys*-LLys-LGln-LThr-LAla-NH_2]	over 15000	5300 (1000)	below 0.4
19	AMTH-Ahx-Abu-[LAla-LArg-LLys*-LLys-LGln-LThr-LAla-NH_2]	over 15000	1600 (700)	below 0.1
20	Adc-Ahx-DAsp*[LArg_6-LAla-LArg-LLys*-LLys-LGln-LThr-LAla-NH_2]-NH_2	23 (4)	2.9 (0.6)	0.1
21	Adc-Ahx-DAsp*[DArg_6-LAla-LArg-LLys*-LLys-LGln-LThr-LAla-NH_2]-NH_2	14 (2)	17 (2)	1
22	Adc-Ahx-DAsp-NH_2	over 15000	over 15000	ND
23	LAla-LArg-LLys-LLys-LGln-LThr-LAla-DArg_6-NH_2	5800 (1800)	over 15000	over 3

* indicates attachment of the notified fragment to the side-chain of the amino acid; **standard error values are given in brackets (N = 2 or more); *** for each compound, selectivity index was calculated as the ratio of K_d values for PKAc and Haspin. For compounds 1-21, the peptidic fragment corresponding to the modified Histone H3(1-7) sequence is shown in square brackets.

The novel conjugates of set B confirmed the aforementioned trends of the structure-affinity relationship. The introduction of Arg_6 motif was crucial for high affinity of compounds, and subnanomolar K_d values could be achieved for Compounds 16 and 17 which are hence more affine towards Haspin than 5-iodotubercidin. Compound 15 possessed K_d value of 170 nM, which was the best result for all novel compounds not incorporating a Arg_6 peptide. Again, acylation of the N-terminus of the Histone H3(1-7)-like peptide caused drop of affinity (K_d value of 5200 for Compound 14 *versus* K_d value of 170 nM for Compound 15). The latter observation might be explained by decrease of the net number of positive charges in the structure of conjugate that are important for binding to basophilic Haspin, as well as by disruption of hydrogen bond developed between N-terminal Ala of the Histone H3(1-7) and Glu613 of Haspin according to co-crystal PDB 4OUC. Importantly, it was demonstrated that chiral spacer (DAsp) is required for correct positioning of the fragments of conjugate to their binding sites in Haspin, as replacement of DAsp with non-chiral chain of approximately same length resulted in sharp decrease of affinity of compounds (K_d value of over 15000 nM for Compound 18 *versus* K_d value of 170 nM for Compound 15).

Despite the fact that in set B, the gain in selectivity of novel conjugates towards Haspin *versus* PKAc as compared to the selectivity index of the reference compound ARC-902 was not strikingly pronounced, the affinity of the most selective Compound 16 was 90-fold higher to Haspin than to PKAc. Again, the positioning of Arg_6 motif at the C-terminus of Histone H3(1-7)-like peptide was extremely important for achieving such selectivity.

Finally, it was confirmed that neither the peptidic part of the conjugates (Compound 23) nor the fragment binding to ATP-site conjugated with linker (Compound 22) revealed significant affinity towards Haspin. The increase of affinity upon conjugation of the peptidic part *via* the linkers and chiral spacer with the Adc was over 6000-fold (i.e., K_d value of 0.88 nM for Compound 17 *versus* K_d value of 5800 nM for Compound 25). The latter fact hence pointed indirectly to the bisubstrate character (*i.e.*, simultaneous association with both substrate-binding sites of Haspin) of the most affine novel conjugates.

2.4.2. Selectivity Studies

Eventually, wide selectivity testing of two novel conjugates was performed toward a panel of 43 kinases. Compounds 15 (final total concentration in the assay of 5 μM) and 16 (final total concentration in the assay of 1 μM) were profiled on the commercial basis at Carna Biosciences using inhibition assays (IMAP assay or Off-chip Mobility Shift Assay). The established inhibition percentages (Table 4) were compared to those obtained for the reference compound ARC-902 (final total concentration in the assay of 1 μM) in the previous studies (performed on the commercial basis at the Division of Signal Transduction Therapy, University of Dundee)[18].

The list of targets chosen for profiling included PKs serving as important players in mitosis (*e.g.*, Aurora, CDK, NEK families) as well as several other PKs (*e.g.*, basophilic Akt, Pim, ROCK families) that had previously been included in the selectivity profiling within the frame of our previous studies. Tyrosine kinase HER2 and acidophilic Ser/Thr PK CK2 were included as the presumable negative controls. As the profiling of Compounds 15 and 16 was performed at relatively high concentrations of the compounds (*i.e.*, compared to their affinities established the displacement assay), it was expected that novel conjugates will inhibit several PKs of the chosen set.

Indeed, Compound 16 inhibited at 1 μM concentration efficiently (i.e., to the extent of 80% or more) most of the basophilic PKs in the panel (including PKs from AGC and CAMK groups, Aurora B and CLK1) with the exception of Auroras A and C and BRSK2. In addition, Compound 16 inhibited efficiently several PKs of CDK family (except CDK7 and CDK9) and NEK family (except NEK2 and NEK7). In general, the selectivity profile revealed by Compound 16 was closely similar to that of the reference compound ARC-902, whereas PKs Aurora B, CDK2/CycA, NEK6, Pim2 and PKCα were even more inhibited by Compound 16 than by ARC-902. Expectedly, acidophilic CDC7, CK2 and PLK family PKs were not inhibited (negative inhibition % values result most likely from the fact that peptide-containing conjugates might serve as reagents reducing the non-specific binding of PKs to the surfaces, and not from activation of the PKs by conjugates). These results showed that the strong positive charge of Arg_6 motif made conjugates overall 'appealing' for basophilic PKs irrespective of other amino acids included in the specific peptidic fragment of the inhibitors.

Compound 15, on the other hand, possessed remarkably more focused selectivity profile even at 5 μM concentration (higher concentration was chosen for screening as Compound 15 was less affine towards Haspin in displacement assay than Compound 16). Out of 43 PKs, only 3 were inhibited to the extent over 80% (Haspin, PKAc and ROCK2); another 3 PKs were inhibited to the extent of 60 to 80% relative to non-inhibited control (CHK1, p70S6K and Pim1). These results indicated that Compound 15 served as a successful example of Haspin-targeting bisubstrate-analogue inhibitors, which not only profited in the aspect of affinity towards Haspin (*i.e.*, from linking of two otherwise weakly binding fragments, Adc and Histone H3(1-7)-like peptide), but also retained Haspin-selectivity conferred by the peptidic fragment derived from the natural protein substrate. This is a remarkable achievement given the reported evidence that conjugation of a target-specific peptide with an additional moiety does not always translate into the conservation of selective properties of the initial fragment(s).[22]

Table 4. PK inhibition profiles for Compounds 15 and 16 (established on commercial basis by Carna Biosciences within this study) and reference compound ARC-902 (reported previously)[18]

PK	PK Group	Compound 15 5 μM	Compound 16 1 μM	ARC-902 1 μM
HER2	TK	-8	-60	-
AKT1 (PKBα)	AGC	46	97	98**
AKT3 (PKBγ)	AGC	28	94	-
AurA	other	-19	48	-
AurB	other	-8	87	-3***
AurC	other	-93	23	-
BRAF	TKL	34*	86*	-
BRSK2 (SAD-A)	CAMK	24	57	-
CDC2 (Cdk1)/CycB1	CMGC	7	99	-
CDC7/ASK	other	-18	-146	-
CDK2/CycA2	CMGC	15	98	12***
CDK2/CycE1	CMGC	-2	88	-
CDK3/CycE1	CMGC	0	74	-
CDK4/CycD3	CMGC	-7	72	-
CDK6/CycD3	CMGC	3	67	-
CDK7/CycH/MAT1	CMGC	-4	-73	-
CDK9/CycT1	CMGC	-1	23	-
CHK1	CAMK	61	102	84***
CHK2	CAMK	46	96	86***
CK2α1/β	other	-5	-19	-4**
CK2α2/β	other	-12	-27	-
CLK1	CMGC	58	102	-
COT (MAP3K8)	STE	38*	-38*	-

GSK3β	CMGC	-3	-11	44**
Haspin	**other**	**102**	**99**	**-**
LATS2	AGC	58	102	-
MSK1	AGC	55	101	98***
NEK1	other	8	84	-
NEK2	other	4	-23	18****
NEK6	other	2	61	6****
NEK7	other	-2	37	42***
NEK9	other	15	65	-
p38α (MAPK14)	other	2	33	21****
p70S6K	AGC	61	100	93***
PIM1	CAMK	73	102	-
PIM2	CAMK	59	102	62**
PKACα	AGC	98	100	89***
PKCα	AGC	51	100	69***
PLK1	other	-9	-84	19**
PLK2	other	7	-56	-
ROCK2	AGC	96	102	100***
RSK1	AGC	11	95	72****
SGK	AGC	11	99	84***

Colour code:

Colour	% inhibition	Colour	% inhibition	Colour	% inhibition
	below 20		40-60		above 80
	20-40		60-80		no data

Final total concentrations of ATP in the assay: * 1 mM; ** 5 μM; *** 20 μM; **** 50 μM; no asterisk, close to K_m(ATP) value for a given PK.

3. Conclusion

In this work, we performed a wide screening of nucleoside mimic-peptide conjugates towards the mitotic protein kinase Haspin. In total, affinity of 48 compounds was evaluated including 6 fluorescent probes and 23 novel compounds comprising peptides derived from the only known physiological substrate of Haspin, Histone H3. The most affine novel conjugate (Compound 16) possessed a subnanomolar K_d value towards Haspin and revealed 90-fold higher affinity towards Haspin than towards the basophilic reference kinase, PKAc. The profiling of two novel conjugates at elevated concentrations (1 μM and 5 μM) towards a panel of 43 PKs (including most important players in mitosis) indicated that a conjugate incorporating a short peptide with Haspin substrate-like sequence from N-terminus of Histone H3 possessed higher Haspin selectivity than its oligoarginine-containing counterpart. Moreover, incorporation of both the Histone H3-like peptide and hexaarginine resulted in loss of Haspin selectivity. Overall, the novel scaffolds generated in this work as well as the established structure-affinity and structure-selectivity relationship will strongly contribute to development of Haspin-targeting selective highly affine probes.

4. Experimental Procedures

4.1. Materials

Chemicals and resins for synthesis were obtained from Iris Biotech, Neosystem, Novabiochem, Caslo, Advanced ChemTech, or AnaSpec. 5-Iodotubercidin was from Cayman Chemicals. PKAc type α (recombinant human protein, full sequence) was a kind gift from Prof. Richard A. Engh (Norwegian Structural Biology Centre, University of Tromsø).

4.2. Synthesis of Conjugates

The novel conjugates were synthesized according to solid phase peptide synthesis procedures using the previously published protocols.[15] After synthesis, the compounds were purified with Schimadzu LC Solution HPLC system (Prominence) using a Gemini C18 reverse-phase column (5 μm, 25 cm×0.46 cm), manual injection and a diode array UV-vis detector (SPD M20A). The high-resolution mass spectra (HRMS) of compounds were measured with Thermo Electron LTQ Orbitrap mass spectrometer.

NanoDrop 2000c (Thermo Scientific) spectrophotometer was used for quantification of the compounds based on the following molar extinction coefficient (ε) values: Adc (15,000 $M^{-1}cm^{-1}$ at 260 nm), AMTH (15,000 $M^{-1}cm^{-1}$ at 340 nm), H9 (4,400 $M^{-1}cm^{-1}$ at 323 nm), PIPY (16,000 $M^{-1}cm^{-1}$ at 286 nm), PYB (16,900 $M^{-1}cm^{-1}$ at 250 nm), TIBI (10,300 $M^{-1}cm^{-1}$ at 300 nm), Cy3B (130,000 $M^{-1}cm^{-1}$ at 558 nm), or TAMRA (80,000 $M^{-1}cm^{-1}$ at 558 nm). The ε values for $_D Arg_9$-NH_2 peptide and Compound 23 were calculated according to literature[23] as 9,200 $M^{-1}cm^{-1}$ and 12,900 $M^{-1}cm^{-1}$ at 214 nm, respectively. The detailed synthetic procedures as well as mass-spectrometry and HPLC data are presented under Supporting Information (Supplementary Methods, Table S2 and Table S3).

4.3. Haspin Production and Purification

Human recombinant Haspin protein (residues 470-798) with a TEV-cleavable N-terminal His_6-tag was produced and purified according to the previously published protocols.[2] The experimental m/z of the protein was confirmed by LC-MS using Agilent LC/MSD TOF system.

4.4. Biochemical Assays with Detection of Fluorescence Polarization/Anisotropy

The fluorescence anisotropy measurements were performed according to the previously published protocols[14] by using PHERAstar microplate reader (BMG Labtech) with an optic module for TAMRA-labeled compounds [ex. 540(20) nm, em. 590(20) and 590(20) nm]. All the solutions of samples were prepared in 384-well low-binding surface microtiter plates (Corning, code 3676). The assay buffer contained 50 mM Hepes (pH 7.5), 150 mM NaCl, 5 mM dithiothreitol and 0.005% Tween-20. GraphPad Prism version 5.0 (GraphPad Software, Inc) was used for data processing and analysis.

4.5. Thermal Shift Assay

Thermal shift assay measurements were performed according to the previously published protocols[24] using a real-time PCR instrument (Mx3005p RT-PCR, Stratagene). The final total concentrations of Haspin and ARCs in the experiments were 2 μM and 12.5 μM, respectively. The measurements were performed in PCR low-profile microplate wells (ABgene). The temperature scan was run from 25 ºC to 95 ºC at 1 ºC/min. GraphPad Prism version 6.0 (GraphPad Software, Inc) and Microsoft Excel version 2007 software were used for data processing and analysis.

Acknowledgements

This work was supported by grants from the Estonian Research Council (PUT0007 and IUT20-17). KK received a Kristjan Jaak stipendium from SA Archimedes. A.C, A.N.B. and SK are grateful for financial support by the SGC, a registered charity (number 1097737) that receives funds from AbbVie, Bayer Pharma AG, Boehringer Ingelheim, the Canada Foundation for Innovation, Genome Canada, GlaxoSmithKline, Janssen, Lilly Canada, the Novartis Research Foundation, the Ontario Ministry of Economic Development and Innovation, Pfizer, Takeda, and the Wellcome Trust [092809/Z/10/Z].

Supporting Information Available: synthesis protocols, structures of all compounds used in this study, HRMS and HPLC data for novel compounds, *etc*. This material is available free of charge *via* the Internet at http://pubs.acs.org.

References

1. Higgins, J. M. (2001) Haspin-like proteins: a new family of evolutionarily conserved putative eukaryotic protein kinases. *Protein Sci. 10*, 1677–1684
2. Eswaran, J., Patnaik, D., Filippakopoulos, P., Wang, F., Stein, R. L., Murray, J. W., Higgins, J. M., Knapp, S. (2009) Structure and functional characterization of the atypical human kinase haspin. *Proc Natl Acad Sci U S A. 106*, 20198–20203
3. Villa, F., Capasso, P., Tortorici, M., Forneris, F., de Marco, A., Mattevi, A., Musacchio, A. (2009) Crystal structure of the catalytic domain of Haspin, an atypical kinase implicated in chromatin organization. *Proc Natl Acad Sci U S A. 106*, 20204–20209
4. Dai, J., Sultan, S., Taylor, S. S., Higgins, J. M. (2005) The kinase haspin is required for mitotic histone H3 Thr 3 phosphorylation and normal metaphase chromosome alignment. *Genes Dev. 19*, 472–488

5. Dodson, C. A., Haq, T., Yeoh, S., Fry, A. M., Bayliss, R. (2013) The structural mechanisms that underpin mitotic kinase activation. *Biochem Soc Trans. 41*, 1037–1041
6. Wang, F., Ulyanova, N. P., Daum, J. R., Patnaik, D., Kateneva, A. V., Gorbsky, G. J, Higgins, J. M. (2012) Haspin inhibitors reveal centromeric functions of Aurora B in chromosome segregation. *J Cell Biol. 199*, 251–268
7. De Antoni, A., Maffini, S., Knapp, S., Musacchio, A., Santaguida, S. (2012) A small-molecule inhibitor of Haspin alters the kinetochore functions of Aurora B. *J Cell Biol. 199*, 269–284
8. Maiolica, A., de Medina-Redondo, M., Schoof, E. M., Chaikuad, A., Villa, F., Gatti, M., Jeganathan, S., Lou, H. J., Novy, K., Hauri, S., Toprak, U. H., Herzog, F., Meraldi, P., Penengo, L., Turk, B. E., Knapp, S., Linding, R., Aebersold, R. (2014) Modulation of the chromatin phosphoproteome by the haspin protein kinase. *Mol Cell Proteomics. 13*, 1724–1740
9. Patnaik, D., Jun Xian, Glicksman, M. A., Cuny, G. D., Stein, R. L., Higgins, J. M. (2008) Identification of small molecule inhibitors of the mitotic kinase haspin by high-throughput screening using a homogeneous time-resolved fluorescence resonance energy transfer assay. *J Biomol Screen. 13*, 1025–1034
10. Uri, A., Lust, M., Vaasa, A., Lavogina, D., Viht, K., Enkvist, E. (2010) Bisubstrate fluorescent probes and biosensors in binding assays for HTS of protein kinase inhibitors. *Biochim Biophys Acta. 1804*, 541–546
11. Lavogina, D., Enkvist, E., Uri, A. (2010) Bisubstrate inhibitors of protein kinases: from principle to practical applications. *ChemMedChem. 5*, 23–34
12. Ekambaram, R., Enkvist, E., Vaasa, A., Kasari, M., Raidaru, G., Knapp, S., Uri, A. (2013) Selective bisubstrate inhibitors with sub-nanomolar affinity for protein kinase Pim-1. *ChemMedChem. 8*, 909–913
13. Lavogina, D., Kalind, K., Bredihhina, J., Hurt, M., Vaasa, A., Kasari, M., Enkvist, E., Raidaru, G., Uri, A. (2012) Conjugates of 5-isoquinolinesulfonylamides and oligo-D-arginine possess high affinity and selectivity towards Rho kinase (ROCK). *Bioorg Med Chem Lett. 22*, 3425–3430
14. Vaasa, A., Viil, I., Enkvist, E., Viht, K., Raidaru, G., Lavogina, D., Uri, A. (2009) High-affinity bisubstrate probe for fluorescence anisotropy binding/displacement assays with protein kinases PKA and ROCK. *Anal Biochem. 385*, 85–93
15. Lavogina, D., Nickl, C. K., Enkvist, E., Raidaru, G., Lust, M., Vaasa, A., Uri, A., Dostmann, W. R. (2010) Adenosine analogue-oligo-arginine conjugates (ARCs) serve as high-affinity inhibitors and fluorescence probes of type I cGMP-dependent protein kinase (PKGIalpha). *Biochim Biophys Acta. 1804*, 1857–1868
16. Lavogina, D., Lust, M., Viil, I., König, N., Raidaru, G., Rogozina, J., Enkvist, E., Uri, A., Bossemeyer, D. (2009) Structural analysis of ARC-type inhibitor (ARC-1034) binding to protein kinase A catalytic subunit and rational design of bisubstrate analogue inhibitors of basophilic protein kinases. *J Med Chem. 52*, 308–321
17. Enkvist, E., Vaasa, A., Kasari, M., Kriisa, M., Ivan, T., Ligi, K., Raidaru, G., Uri, A. (2011) Protein-induced long lifetime luminescence of nonmetal probes. *ACS Chem Biol. 6*, 1052–1062
18. Enkvist, E., Lavogina, D., Raidaru, G., Vaasa, A., Viil, I., Lust, M., Viht, K., Uri, A. (2006) Conjugation of adenosine and hexa-(D-arginine) leads to a nanomolar bisubstrate-analog inhibitor of basophilic protein kinases. *J Med Chem. 49*, 7150–7159
19. Räägel, H., Lust, M., Uri, A., Pooga, M. (2008) Adenosine-oligoarginine conjugate, a novel bisubstrate inhibitor, effectively dissociates the actin cytoskeleton. *FEBS J. 275*, 3608–3624
20. Lavogina, D., Budu, A., Enkvist, E., Hopp, C. S., Baker, D. A., Langsley, G., Garcia, C. R., Uri, A. (2014) Targeting Plasmodium falciparum protein kinases with adenosine analogue-oligoarginine conjugates. *Exp Parasitol. 138*, 55–62
21. Futaki, S., Hirose, H., Nakase, I. (2013) Arginine-rich peptides: methods of translocation through biological membranes. *Curr Pharm Des. 19*, 2863–2868
22. Livnah, N., Yechezkel, T., Salitra, Y., Perlmutter, B., Ohne, O., Cohen, I., Litman, P., Senderowitz, H. (2004) Protein Kinase Inhibitors Comprising ATP Mimetics Conjugated to Peptides or Peptidomimetics. *EP1416934*
23. Kuipers, B. J., Gruppen, H. (2007) Prediction of molar extinction coefficients of proteins and peptides using UV absorption of the constituent amino acids at 214 nm to enable quantitative reverse phase high-performance liquid chromatography-mass spectrometry analysis. *J Agric Food Chem. 55*, 5445–5451

24. Fedorov, O., Niesen, F. H., Knapp, S. (2012) Kinase inhibitor selectivity profiling using differential scanning fluorimetry. *Methods Mol Biol. 795*, 109–118